

14p

NTIS HC \$3.00

X-641-72-435

PREPRINT

NASA TM X

66117

# SCANNING-ANGLE DISTRIBUTION OF PLANETARY ALBEDO GAMMA RAYS: A SIMPLE MODEL

F. W. STECKER

(NASA-TM-X-66117) SCANNING-ANGLE  
DISTRIBUTION OF PLANETARY ALBEDO GRAMMA  
RAYS: A SIMPLE MODEL F.W. Stecker (NASA)  
Nov. 1972 13 p CSCL 03B

N73-12874

Unclas  
49142

G3/29

NOVEMBER 1972



— GODDARD SPACE FLIGHT CENTER —  
GREENBELT, MARYLAND

SCANNING-ANGLE DISTRIBUTION OF PLANETARY  
ALBEDO GAMMA-RAYS: A SIMPLE MODEL

F. W. Stecker  
Theoretical Studies Branch  
Laboratory for Space Physics  
NASA/Goddard Space Flight Center  
Greenbelt, Maryland

**Abstract:** A simple model for calculating the planetary albedo scanning angle distribution above 100 MeV is discussed and the results are compared with present observations.

It is now within the realm of technological feasibility to study the structure of a planet's atmosphere and (indirectly) its magnetosphere by means of a high-energy, high-resolution gamma-ray detector such as a large spark chamber or gas Cerenkov counter mounted on an orbiting satellite (see reviews by Kraushaar<sup>1</sup> and Kniffen<sup>2</sup>). The bulk of the radiation at energies greater than 100 Mev, at the limb of the planet, originates from the decay of  $\pi^0$  mesons produced by cosmic-rays interacting with nuclei in the planet's atmosphere. Thus, by scanning the planet from the sub-satellite point to the limb with a high-resolution detector one may unfold from the angular distribution of the gamma-ray flux, the mean total baryonic scale height of the atmosphere. In a planet possessing a magnetosphere, lower energy cosmic-rays may not penetrate to the atmosphere and in such regions of low magnetic latitude, there will be a minimum in the gamma-ray flux whereas in high penetration regions such as

magnetic poles, maxima should occur. In this paper, a simple model of a planet with an isothermal atmosphere is considered, neglecting possible geomagnetic effects. For purposes of some comparison with existing data, a "non-magnetic" earth is considered.

The geometry of the model is shown in figure 1. The satellite is located at point S at an altitude  $a=5 \times 10^7$  cm from the subsatellite point on the surface. We consider a cosmic-ray primary entering the atmosphere from a point P and colliding with an atmospheric gas nucleus at point C. The resulting secondary gamma-ray is emitted at C and travels to S where it is detected.  $R_e$  is the radius of the earth; taken to be  $6.37 \times 10^8$  cm and h is the height of the collision point C above the surface. The cosmic-ray path makes an angle  $\chi$  with the vertical at C where  $0 < \chi < \chi_M$   $\chi_M$  being the maximum allowed angle as shown.

$$\chi_M(h) = \sin^{-1} [R_e / (R_e + h)] \quad (1)$$

The angle that the line CS makes with the vertical at C is denoted by  $\chi_a$ . Thus, we may write h as a function of  $\chi_a$ , a, and the scanning angle  $\psi$  so that  $h(\chi_a)$  with  $\psi$  and a given is

$$h(\chi_a; \psi, a) = R_e \left[ \left(1 + \frac{a}{R_e}\right) \frac{\sin \psi}{\sin \chi_a} - 1 \right] \quad (2)$$

The parameters  $s$  and  $t$  shown in figure 1 are given by the relations

$$s = (R_e + h) \sin \chi \quad (3)$$

$$\text{and } t = (R_e + a) \sin \psi .$$

We denote by  $\mu$ , the cosine of the angle between the incoming cosmic ray at C and the outgoing gamma-ray.

It then follows that

$$\mu = \cos \chi_a \cos \chi + \sin \chi_a \sin \chi \cos \alpha ,$$

$\alpha$  being the angle in the plane tangent to the vertical at c.

If we assume isotropic production of pions in the cms system, the angular distribution of photons in the laboratory system is given by <sup>3</sup>

$$G(\mu; E_p) = \frac{1}{\gamma_c (1 - \beta_c \mu)} \quad (4)$$

where  $\gamma_c$  is the cms Lorentz factor and  $\beta_c c$  the cms velocity of the cosmic-ray-nucleus system. Here, for simplicity, we assume that the baryons in the nucleus act as if they are unbound at these energies ( $>1\text{GeV}$ ) so that

$$G(\mu; E_p) = \left\{ \left[ \frac{E_p/M+1}{2} \right]^{\frac{1}{2}} \left[ 1 - \left( \frac{E_p/M+1}{E_p/M+1} \mu \right) \right] \right\}^{-1} \quad (5)$$

where  $M$  is the nucleon rest mass ( $0.938\text{GeV}$ ). We consider here an isothermal atmosphere with density

$$\rho = \rho_0 e^{-h/H} \quad (6)$$

where  $\rho_0 = 1.225 \times 10^{-3} \text{ g.cm}^{-3}$  and the scale height  $H = 10^6 \text{ cm}$ .

The incoming cosmic-ray intensity is taken to be

$$K E_p^{-2.2} (\text{cm}^2 \cdot \text{s} \cdot \text{sr} \cdot \text{GeV})^{-1}, \quad K = 0.437. \quad (7)$$

The cosmic-rays are taken to have an absorption mean-free-path  $\Lambda_p = 120 \text{ g/cm}^2$  and the photon absorption mean-free-path is taken to be  $\Lambda_\gamma = 60 \text{ g/cm}^2$ .

Thus, the cosmic-ray intensity at C is given by

$$I_C(E_p; \chi, \psi, a) = K E_p^{-2.2} i(\chi; \psi, a) \quad (8)$$

$$\text{where } i(\chi; \psi, a) = \exp \left\{ - \frac{\rho_0 s}{\Lambda_p} \int_0^\chi e^{-(s \csc \lambda - R_e)/H} \csc^2 \lambda d\lambda \right\}$$

The resulting photons are attenuated by a factor  $e^{-\eta}$  where

$$\eta = \frac{\rho_0 t}{\Lambda_\gamma} \int_\psi^{\pi-\chi_a} d\phi \csc^2 \phi e^{-(t \csc \phi - R_e)/H} \quad (9)$$

We assume the production cross section for  $\pi^0$ -mesons in the atmosphere to be of the form<sup>4</sup>

$$\sigma_\pi(E_p) \approx 3.5 \times 10^{-25} E_p^{0.5} (\text{GeV}) \quad (10)$$

Then, the gamma-ray intensity from pion decay

( $E_\gamma \geq 70 \text{ MeV}$ ) reaching the satellite is given by

$$I(\psi, a) = 4N\rho_0 K t \int_0^{\pi-\psi} \csc^2 \chi_a d\chi_a \int_0^\pi d\alpha \int_{-|\cos \chi_M|}^1 d(\cos \chi) \times \quad (11)$$

$$\times \int_{E_C}^{E_{\text{MAX}}} dE_p e^{-(\eta + \frac{h}{H})} E_p^{-2.2} G(\mu; E_p) \sigma_{\pi^0}(E_p) i(\chi; \psi, a)$$

where  $E_C$ , the lower cutoff energy is, in general, a function of geomagnetic latitude, but is here taken to be 2 GeV,  $E_{\text{MAX}}$  for purposes of numerical calculation is taken to be 10 GeV and  $N$  is Avagadro's constant.

The results obtained from a numerical evaluation of equation (11) are shown in the polar diagram in figure 2 with the earth superimposed to scale. They show a strong peaking in intensity toward the horizon due mainly to the forwardly-directed gamma-rays (see equation (4)). A more realistic pion-production model than the cms-isotropic model used here would result in an even stronger "limb-brightening" effect which increases with energy. Above the horizon angle, the flux drops rapidly to zero as the atmosphere disappears; below the horizon angle, the atmosphere becomes optically thick and the flux distribution approximates a  $\sec\psi$ -law as indicated by the dashed line in figure 2.

In figure 3, the calculated results are compared with some of those obtained on OSO-3 (Ref. 5). The calculated distribution (dashed line) is folded in with the angular-response function of the OSO-3 detector, generating the solid line. Some of the data given by Borken<sup>5</sup> are shown for comparison. The agreement in intensity is probably fortuitous; a higher average cutoff energy would have reduced the calculated flux and the absolute sensitivity of the detector has since been revised (Kraushaar et al. Ref. 6). Later data on  $I(\psi)$  (Kraushaar, et al. Ref. 6), show a somewhat more pronounced limb-brightening effect as would be expected with a higher average geomagnetic cutoff and a more anisotropic cms-pion distribution. However there is generally good agreement between the OSO-3 data and the calculated  $I(\psi)$  given here. Also in support of the model given here, rough data obtained by OSO-3 on the hardness of the spectrum of gamma-rays at the limb indicates a  $\pi^0$ -decay

origin. The softer spectrum obtained for  $\psi \approx 0$  may indicate an admixture of cascade radiation but it should also be kept in mind that backward pions produce gamma-rays with lower average energy than forward pions (the direction referring to the cms system). Also, as Borken points out<sup>5</sup>, only multiply degraded cascade photons should contribute to the nadir flux and these are, in general, below the threshold energy of the detector. In addition, Borken points out that a cascade flux should have a secondary maximum at the nadir, contrary to the observations. The problem of the nadir flux does not have an easy solution and must be treated by more sophisticated methods.

Unfortunately, because of the limitations in the resolution of the OSO-3 detector, the model presented here may not provide a unique fit to the observations. It can clearly be seen in figure 3 that the shape of the observed curve is resolution dominated and that the broad peak observed just below the horizon is caused by a smearing-out of a narrow bright horizon flux (dashed line). There is clearly room for improvement in both theory and observation but reasonably good results for the simple model presented here are encouraging.

## REFERENCES:

1. Kraushaar, W. L., Astronautics and Aeronautics, p. 28, July 1969.
2. Kniffen, D. Gamma-Ray Telescopes in Cosmic Gamma Rays, F. W. Stecker, Mono Book Corp., Baltimore, 1971.
3. Baldin, A. M., V. I. Goldanskii and I. L. Rozental Kinematics of Nuclear Reactions, Oxford, London, 1961 (Trans. of Kinematika Yadernykh Reaktsii, Moscow 1959).
4. Muirhead, H., The Physics of Elementary Particles, Pergamon Press, New York 1965.
5. Borken, R. A., Study by Satellite of Gamma Rays from the Earth, S. B. Thesis, Massachusetts Institute of Technology, June 1968.
6. Kraushaar, W. L., G. W. Clark, G. P. Garmire, R. Borken, P. Higbie, C. Leong and T. Thorsos, Astrophysical Journal 177, 341, 1972.



**ACKNOWLEDGMENTS:**

I wish to thank Dr. K. Maeda for helpful comments and important suggestions, Dr. G. W. Clark and Dr. R. J. Borken for communicating O60-3 results and helpful discussions and Mr. E. Victor and Mr. P. Smidinger for programming the numerical calculations.

**FIGURE CAPTIONS:**

Figure 1. Geometry of the atmospheric gamma-ray model as discussed in the text.

Figure 2. Polar diagram of calculated  $I(\psi)$  centered on satellite detector with earth below shown to scale.

Figure 3. Comparison of calculated results with OSO-3 observations.

# GEOMETRY OF ATMOSPHERIC $\gamma$ -RAY PROBLEM

FIG. 1

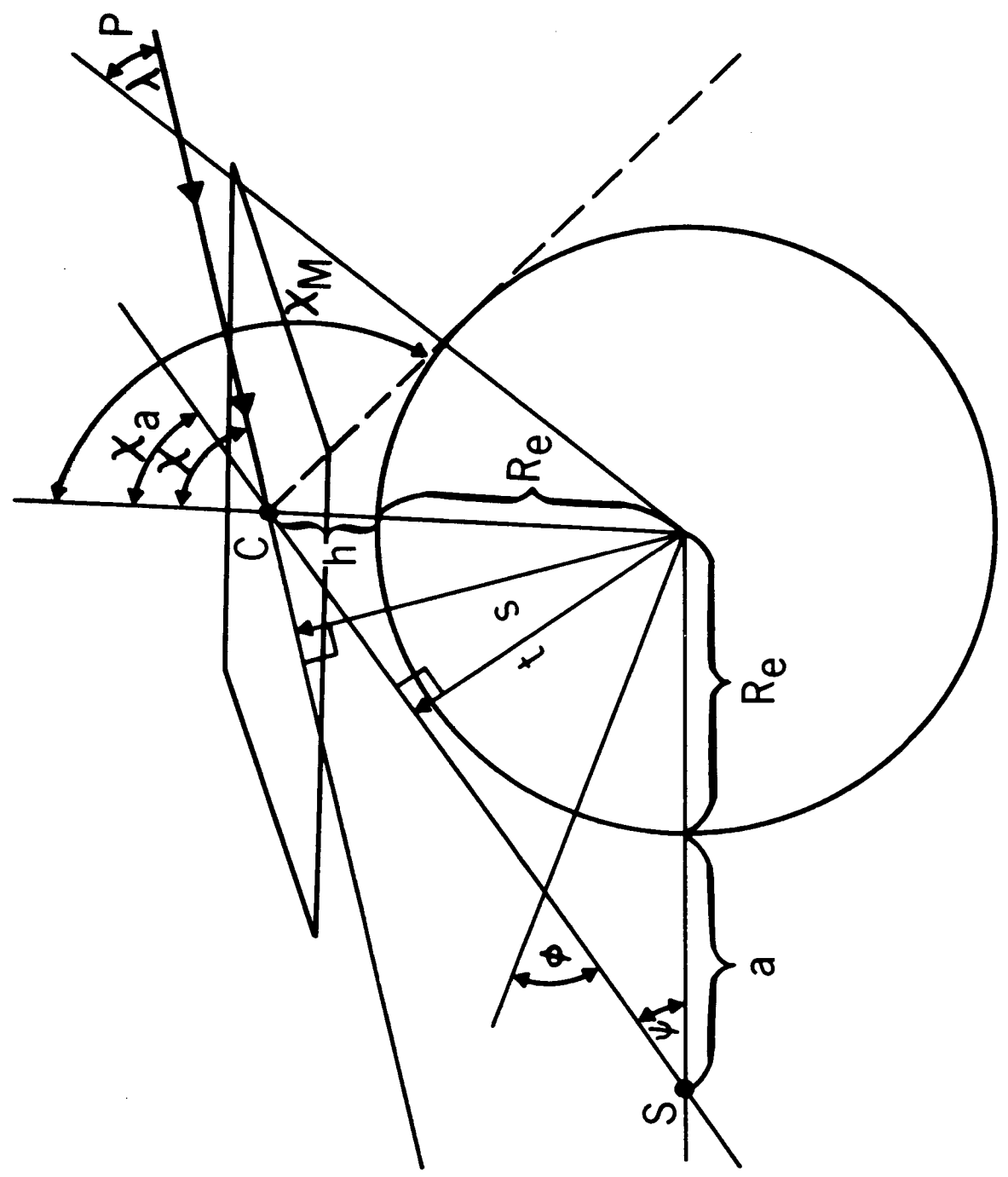


FIG. 2

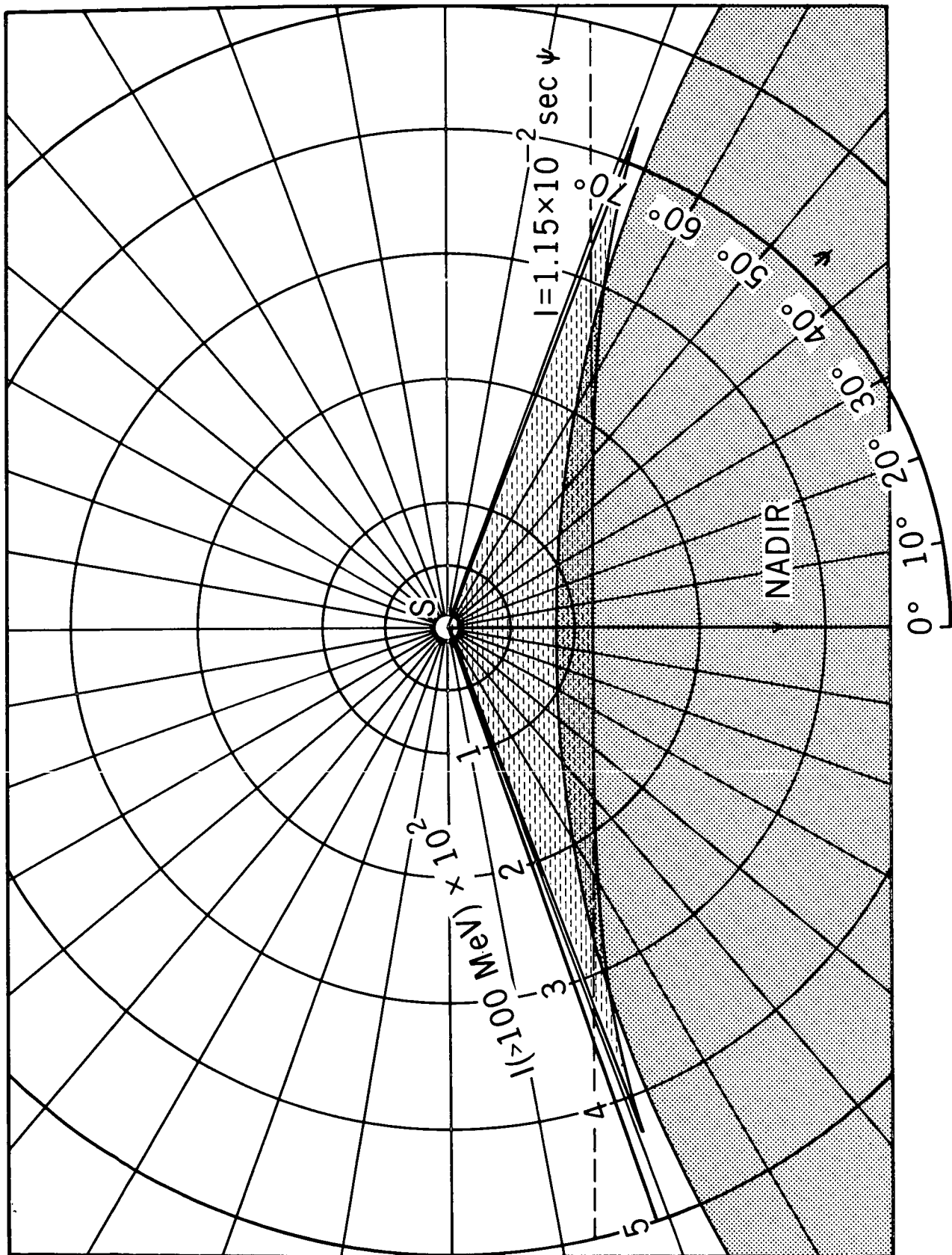


FIG. 3

